Surface & Coatings Technology 306 (2016) 11–15

Contents lists available at ScienceDirect

Surface & Coatings Technology

journal homepage: www.elsevier.com/locate/surfcoat

Hafnium-implanted WE43 magnesium alloy for enhanced corrosion protection and biocompatibility

Weihong Jin, Guosong Wu, Ang Gao, Hongqing Feng, Xiang Peng, Paul K. Chu *

Department of Physics and Materials Science, City University of Hong Kong, Tat Chee Avenue, Kowloon, Hong Kong, China

ARTICLE INFO

Article history:
Received 1 December 2015
Revised 20 February 2016
Accepted in revised form 23 February 2016
Available online 26 February 2016

Keywords:
Magnesium
Ion implantation
Corrosion
Biocompatibility

ABSTRACT

Hafnium (Hf) ion implantation is conducted to improve the corrosion resistance and biocompatibility of WE43 magnesium alloy. The surface composition, corrosion behavior, as well as *in vitro* cell adhesion and cytotoxicity are evaluated. The implanted layer consists of mainly Hf and Mg oxide and Hf ion implantation retards the deterioration of the WE43 magnesium alloy in simulated body fluids. The Hf-implanted WE43 magnesium alloy also shows good cell attachment and negligible cytotoxicity.

1. Introduction

Magnesium and its alloys have aroused much attention due to their promising application to temporary biomedical implants including orthopedic implants [1,2] and cardiovascular stents [3,4]. The WE43 magnesium alloy is one of the attractive biomedical rare-earth magnesium alloys without potentially toxic aluminum [5,6] and addition of small quantities of Nd and Y has been observed to improve the mechanical properties and corrosion resistance of magnesium alloys [7,8]. Owing to the natural biodegradability of magnesium-based alloys under physiological conditions, a follow-up surgery to remove the implant can be avoided after tissue healing [9]. The ideal biodegradable candidate should allow sufficient time for the tissues to heal or grow before losing the mechanical integrity in the dissolution process and simultaneously be biocompatible with the human body. Unfortunately, degradation of magnesium-based alloys in the aggressive physiological environment is quite fast and sometimes unpredictable often leading to premature mechanical failure of the implant before the tissues have time to heal [10]. Fast degradation of Mg and Mg alloys also results in excessive hydrogen evolution, released metal ions, localized alkaline pH condition, and corrosion product formation [11], which may affect recovery of the surrounding tissues and must be controlled. Consequently, it is crucial to improve the corrosion resistance of magnesium alloys and minimize adversary biological reactions in order that the materials can be used clinically.

Surface treatment is a practical and economical strategy to enhance the corrosion resistance and biocompatibility of magnesium-based alloys [12,13] and in particular, ion implantation has several advantages such as no change of the geometric dimensions of the treated specimens, no layer delamination, and precise control of the ion fluence. Hence, ion implantation has been widely implemented to improve the surface properties of materials [14–17]. In biomedical applications, biosafety is also very important and so the choice of the implanted element is limited to those that can improve the corrosion resistance and do not compromise the biological properties. In this respect, hafnium (Hf) belongs to the same chemical group as titanium and zirconium in the periodic table and is expected to provide good corrosion resistance and biocompatibility [18,19]. Hf-based material have been shown to have good anticorrosion properties due to the formation of HfO_2 [20,21] and new Ti alloys containing non-toxic Hf have been developed for biomedical applications [22–24]. However, there have been few studies pertaining to the use of Hf ion implantation to improve the surface properties of magnesium alloys. In this work, Hf is implanted into the WE43 Mg alloy to simultaneously improve the corrosion resistance and biocompatibility.

2. Experimental details

The 10 mm × 10 mm × 2 mm specimens were prepared from the as-cast WE43 magnesium alloy. Prior to ion implantation, the samples were ground successively with 400–1200 grit SiC abrasive papers, ultrasonically rinsed in ethanol for 15 min, and dried in air. Hf ion implantation was conducted on a metal ion implanter equipped with a Hf cathodic arc source (HEMII-80, Plasma Technology Ltd., Hong Kong SAR) for 3 h at an accelerating voltage of 30 kV and base pressure of 4.0×10^{-4} Pa. The ion current was 5 mA and ion fluence was 8×10^{17} cm^{-2}. X-ray photoelectron spectroscopy (XPS, PHI 5802,

* Corresponding author.
E-mail address: paul.chu@cityu.edu.hk (P.K. Chu).

http://dx.doi.org/10.1016/j.surfcoat.2016.02.055
0257-8972/

Physical Electronics, Inc., USA equipped with an Al K_α source) was performed to determine the elemental depth profiles and chemical states of the HWE sample. The sputtering rate was estimated to be 8.0 nm/min based on a SiO_2 reference.

The electrochemical experiments were performed in the simulated body fluid (SBF) at 37 °C on an electrochemical workstation (Zennium, Zahner, Germany) equipped with a three-electrode cell. All the potentials were referred to SCE if not specified otherwise. The SBF solution was prepared using reagent grade chemicals according to the method described by Kokubo [25]. 1 cm^2 of the sample surface was exposed to the solution during the electrochemical measurements. Prior to conducting electrochemical impedance spectroscopy (EIS), the samples were immersed in the solution for 5 min. EIS was conducted at the open circuit potential (OCP) from 100 kHz to 100 mHz and potentiodynamic polarization was subsequently carried out at a scanning rate of 1 mV s^{-1} from −350 mV and 450 mV with respect to the OCP.

To further investigate corrosion on the untreated and implanted WE43, the specimens with an exposed area of 1 cm^2 were also immersed in 20 mL of SBF at 37 °C for 1 day. After rinsing with deionized water and drying in air, the surface morphology and composition before and after immersion were determined by scanning electron microscopy (SEM, JSM-820, JEOL Ltd., Japan) equipped with energy dispersive X-ray spectroscopy (EDS, INCAx-sight, Oxford Instruments, UK). The morphology of the cross-sections after immersion was also examined by SEM and EDS. The biological assessment including direct cell adhesion and indirect cytotoxicity evaluation was performed according to the methods described in our previous paper [26].

3. Results and discussion

Fig. 1 shows that Hf ion implantation produces a surface layer mainly composed of Hf and Mg oxide in addition to a small amount of metallic Hf [27–29]. The oxide layer is expected to protect the substrate from corrosive attack. The polarization curves acquired from WE43 and Hf-implanted WE43 (HWE43) in SBF are shown in Fig. 2 and the corrosion current density (I_{corr}) is determined by Tafel extrapolation of the cathodic polarization curve. HWE43 exhibits much smaller I_{corr} (40.0 ± 1.2 μA cm^{-2}) than WE43 (625.7 ± 45.5 μA cm^{-2}). The smaller the corrosion current density, the less is surface corrosion. The polarization results reveal that degradation of the WE43 magnesium alloy is greatly retarded by Hf ion implantation. The Nyquist plots acquired from WE43 and HWE43 in SBF are shown in Fig. 3 to reveal more details about the corrosion process. HWE43 shows a larger capacitive loop at high and medium/low frequencies, suggesting that the corrosion resistance of

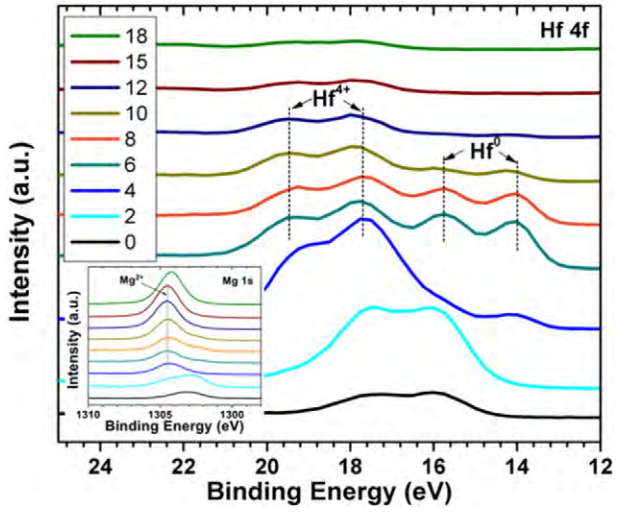

Fig. 1. High-resolution XPS spectra of Hf 4f and Mg 1s acquired at different sputtering time from HWE43.

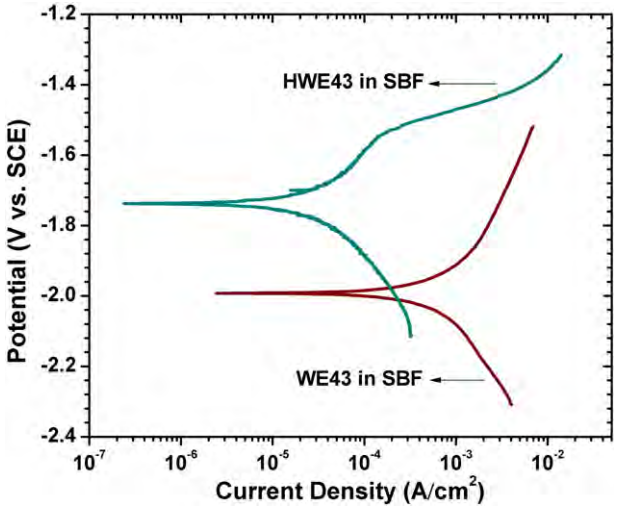

Fig. 2. Polarization curves of WE43 and HWE43 in SBF.

the WE43 magnesium alloy is improved by Hf ion implantation. The equivalent circuits with two and three time constants as shown in Fig. 3 are applied to fit the experimental EIS data without and with an inductive arc, respectively. Zhao et al. [28] and Jamesh et al. [16] have used similar models to explain the corrosion behavior of the bare and implanted WE43 magnesium alloy. R_s corresponds to the solution resistance between the reference electrode and sample. CPE_1 is the capacitance of the oxidized surface layer or corrosion products and R_1 is the corresponding resistance. CPE_2 represents the double layer capacitance at the electrolyte/substrate surface and R_2 is the relevant charge transfer resistance. The inductive loop in the equivalent circuit is possibly associated with adsorption of the corrosion products and R_L represents the corresponding resistance. HWE43 exhibits a large increase in the resistance against mass transportation, R_1, (from 10.8 Ω cm^2 to 1315 Ω cm^2) and charge transfer resistance, R_2, (from 49.6 Ω cm^2 to 1564 Ω cm^2) further indicating that corrosion on HWE43 is mitigated. The obviously larger R_1 and R_2 of HWE43 are attributed to the surface layer containing Hf and Mg oxide formed by Hf ion implantation.

The backscattered electron (BSE) images in Fig. 4 show that after immersion for 1 day in SBF, the corroded area on HWE43 is smaller and there are less cracks on the surface. Smaller amounts of Ca and P but larger amount of Mg are detected from the surface corrosion layer of HWE43 according to EDS. The cross-sectional BSE images in Fig. 5

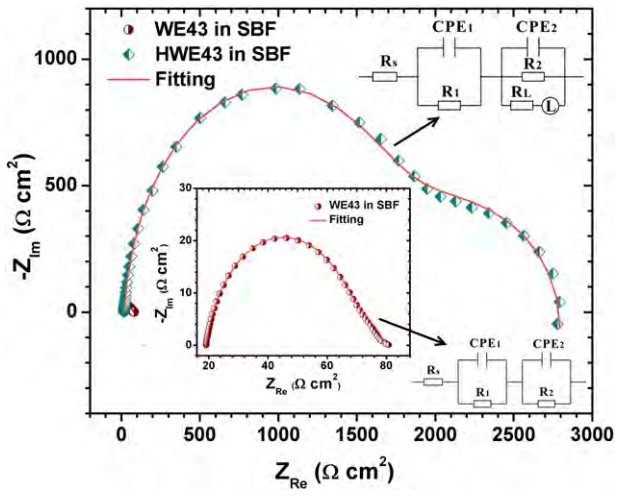

Fig. 3. Nyquist plots of WE43 and HWE43 in SBF. The two corresponding equivalent circuits are used to fit the EIS data.

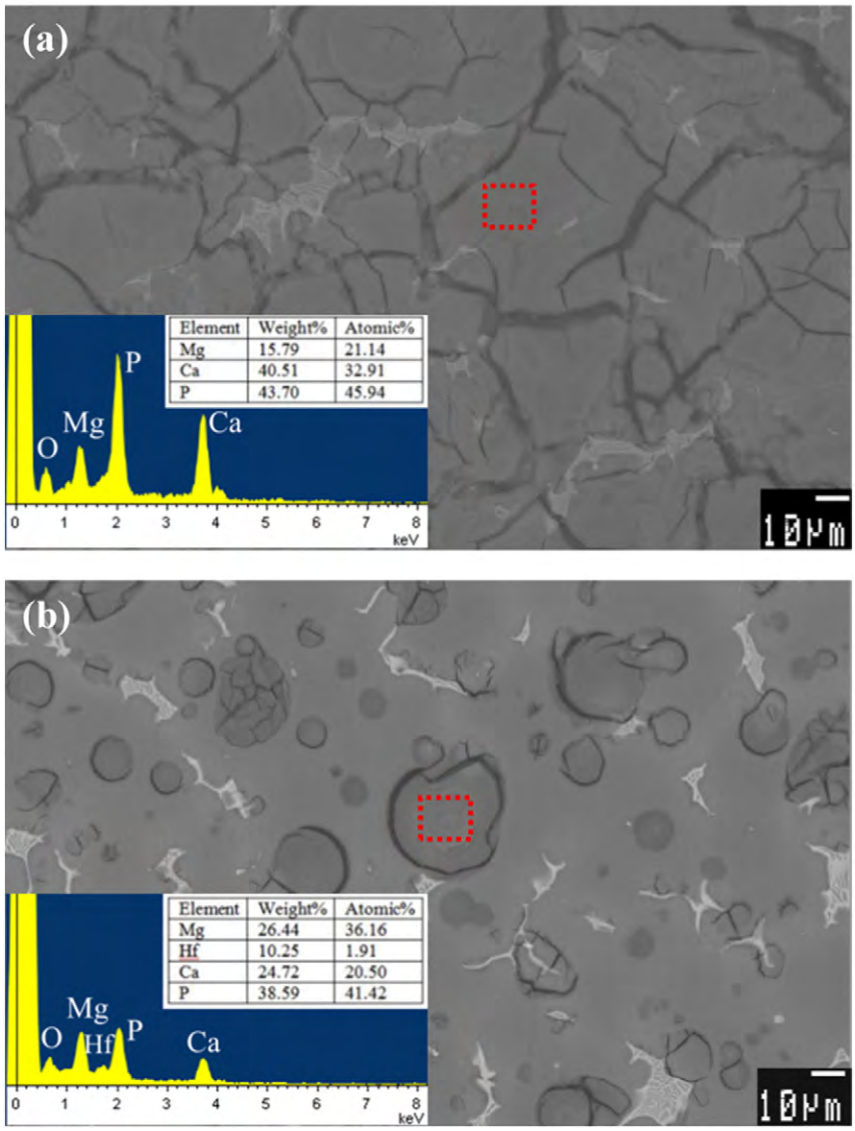

Fig. 4. BSE surface images with the corresponding EDS analysis of WE43 and HWE43 after immersion in SBF for 1 day.

disclose that the corrosion layer on the untreated WE43 sample has a thickness of 27.2 to 62.9 μm, whereas that on HWE43 is less than 12.3 μm. In addition, the untreated WE43 sample has more cracks which provide the paths for the corrosive medium to penetrate through the loose corrosion product layer into the substrate resulting in further degradation of the magnesium substrate. Our results show that the barrier layer formed by Hf ion implantation provides good protection for the substrate in SBF.

After immersion of the untreated WE43 Mg alloy in the corrosive solution, corrosion occurs to the magnesium matrix (Eq. (1)) adjacent to the second phase which has a nobler potential and is less reactive than the magnesium matrix [30]. Insoluble magnesium hydroxide is then formed in the local corroded regions (Eq. (3)).

$$Mg(s) \rightarrow Mg^{2+}(aq) + 2e\text{-(anodic reaction)} \quad (1)$$

$$2H_2O(aq) + 2e\text{-} \rightarrow H_2(g) + 2\,OH^-(aq)\text{(cathodic reaction)} \quad (2)$$

$$Mg^{2+}(aq) + 2OH^-(aq) \rightarrow Mg(OH)_2(s)\ \text{(product formation)} \quad (3)$$

$$Mg(s) + 2H_2O(aq) \rightarrow Mg(OH)_2(s) + H_2(g)\ s\text{(overall reaction)}. \quad (4)$$

The solution can quickly penetrate into the metallic substrate through the product layer with a very loose structure. Therefore, the metallic substrate is continuously consumed by the corrosive electrolyte and a high dissolution rate is expected from the untreated WE43 magnesium alloy. With regard to the HWE43 magnesium alloy, the surface is covered by the implanted layer mainly containing relatively inert Hf oxide and MgO. The corrosive species can only reach the substrate through few unprotected regions. Consequently, the surface layer composed of protective Hf oxide and MgO formed by the Hf ion implantation provides good protection against attack by the corrosive media.

Compared to the high cell cytotoxicity of the untreated WE43 magnesium, the cell viability of the MC3T3-E1 pre-osteoblasts is very good at 95% after the HWE43 extract has been cultured for 3 days, as shown in Fig. 6. The good results reveal that HWE43 has negligible cell cytotoxicity and cells proliferate well during incubation. The number of MC3T3-E1 cells attached to HWE43 is much larger than that to the untreated WE43 sample. Additionally, the MC3T3-E1 cells seeded on HWE43 after incubation for 5 h exhibit better spreading with a good shape. The enhanced corrosion resistance provides a relatively stable environment allowing better initial cell attachment and ensuing cell growth.

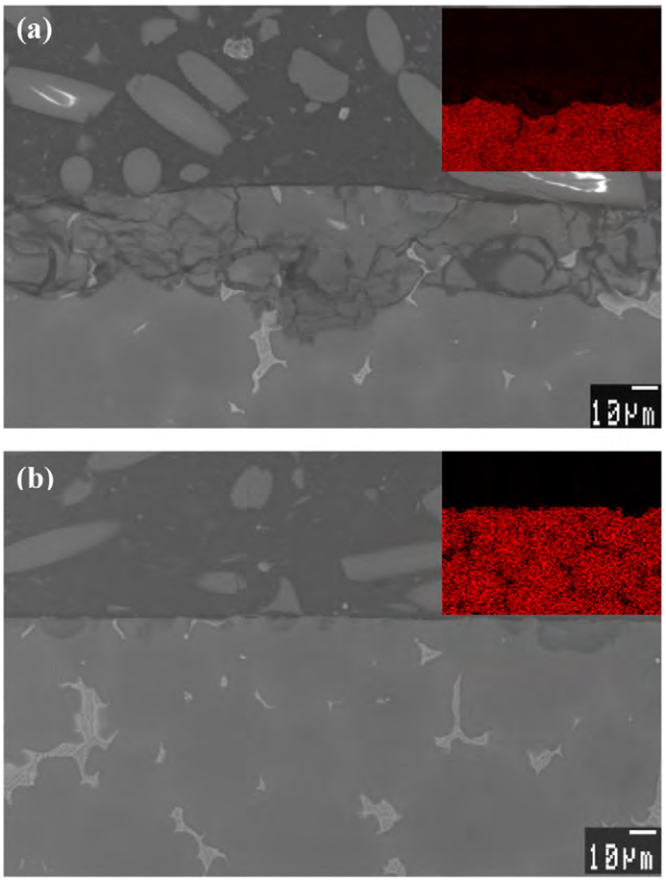

Fig. 5. BSE cross-sectional images with the corresponding EDS maps of WE43 and HWE43 after immersion in SBF for 1 day.

4. Conclusion

A surface layer containing Hf and Mg oxide is produced on WE43 magnesium alloy by Hf ion implantation. The Hf-implanted sample (HWE43) exhibits a smaller corrosion current density, larger charge transfer resistance, and bigger mass transportation resistance in the simulated body fluid (SBF). A loose and thick corrosion product layer is formed on the untreated WE43 magnesium alloy after immersion in SBF for 1 day, but only a few pits allowing shallow penetration of the corrosion medium into the magnesium alloy substrate are observed from HWE43. Moreover, HWE43 shows good cell adhesion and negligible cytotoxicity.

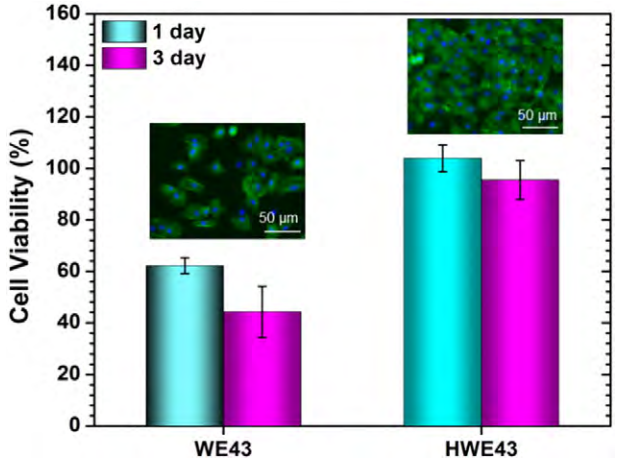

Fig. 6. *In vitro* cell viability of the MC3T3-E1 pre-osteoblasts cultured with the extracted medium from WE43 and HWE43 at time points of 1 and 3 days and fluorescent images of the MC3T3-E1 pre-osteoblasts after incubation on WE43 and HWE43 for 5 h.

Acknowledgments

This work was financially supported by Hong Kong Research Grants Council (RGC) General Research Funds (GRF) Nos. CityU 112212 and 11301215 as well as City University of Hong Kong Strategic Research Grant (SRG) No. 7004188.

References

[1] F. Witte, J. Fischer, J. Nellesen, H.A. Crostack, V. Kaese, A. Pisch, F. Beckmann, H. Windhagen, In vitro and in vivo corrosion measurements of magnesium alloys, Biomaterials 27 (2006) 1013–1018.
[2] F. Witte, V. Kaese, H. Haferkamp, E. Switzer, A. Meyer-Lindenberg, C.J. Wirth, H. Windhagen, In vivo corrosion of four magnesium alloys and the associated bone response, Biomaterials 26 (2005) 3557–3563.
[3] R. Erbel, C. Di Mario, J. Bartunek, J. Bonnier, B. de Bruyne, F.R. Eberli, P. Erne, M. Haude, B. Heublein, M. Horrigan, C. Ilsley, D. Bose, J. Koolen, T.F. Luscher, N. Weissman, R. Waksman, P.A. Investigators, Temporary scaffolding of coronary arteries with bioabsorbable magnesium stents: a prospective, non-randomised multicentre trial, Lancet 369 (2007) 1869–1875.
[4] R. Waksman, R. Pakala, P.K. Kuchulakanti, R. Baffour, D. Hellinga, R. Seabron, F.O. Tio, E. Wittchow, S. Hartwig, C. Harder, R. Rohde, B. Heublein, A. Andreae, K.H. Waldmann, A. Haverich, Safety and efficacy of bioabsorbable magnesium alloy stents in porcine coronary arteries, Catheter. Cardiovasc. Interv. 68 (2006) 607–617.
[5] C. Di Mario, H. Griffiths, O. Goktekin, N. Peeters, J. Verbist, M. Bosiers, K. Deloose, B. Heublein, R. Rohde, V. Kasese, C. Ilsley, R. Erbel, Drug-eluting bioabsorbable magnesium stent, J. Interv. Cardiol. 17 (2004) 391–395.
[6] X. Gu, Y. Zheng, Y. Cheng, S. Zhong, T. Xi, In vitro corrosion and biocompatibility of binary magnesium alloys, Biomaterials 30 (2009) 484–498.
[7] T. Zhang, G. Meng, Y. Shao, Z. Cui, F. Wang, Corrosion of hot extrusion AZ91 magnesium alloy. Part II: effect of rare earth element neodymium (Nd) on the corrosion behavior of extruded alloy, Corros. Sci. 53 (2011) 2934–2942.
[8] L.L. Rokhlin, Magnesium Alloys Containing Rare Earth Metals: Structure and Properties, Taylor and Francis, London, 2003.
[9] F. Witte, N. Hort, C. Vogt, S. Cohen, K.U. Kainer, R. Willumeit, F. Feyerabend, Degradable biomaterials based on magnesium corrosion, Curr. Opin. Solid State Mater. Sci. 12 (2008) 63–72.
[10] M.P. Staiger, A.M. Pietak, J. Huadmai, G. Dias, Magnesium and its alloys as orthopedic biomaterials: a review, Biomaterials 27 (2006) 1728–1734.
[11] G. Song, Control of biodegradation of biocompatable magnesium alloys, Corros. Sci. 49 (2007) 1696–1701.
[12] H. Hornberger, S. Virtanen, A.R. Boccaccini, Biomedical coatings on magnesium alloys — a review, Acta Biomater. 8 (2012) 2442–2455.
[13] G. Wu, J.M. Ibrahim, P.K. Chu, Surface design of biodegradable magnesium alloys — a review, Surf. Coat. Technol. 233 (2013) 2–12.
[14] Y. Zhao, K.W.K. Yeung, P.K. Chu, Functionalization of biomedical materials using plasma and related technologies, Appl. Surf. Sci. 310 (2014) 11–18.
[15] G. Wu, R. Xu, K. Feng, S. Wu, Z. Wu, G. Sun, G. Zheng, G. Li, P.K. Chu, Retardation of surface corrosion of biodegradable magnesium-based materials by aluminum ion implantation, Appl. Surf. Sci. 258 (2012) 7651–7657.
[16] M.I. Jamesh, G. Wu, Y. Zhao, W. Jin, D.R. McKenzie, M.M.M. Bilek, P.K. Chu, Effects of zirconium and nitrogen plasma immersion ion implantation on the electrochemical corrosion behavior of Mg–Y–RE alloy in simulated body fluid and cell culture medium, Corros. Sci. 86 (2014) 239–251.
[17] Y. Qiao, W. Zhang, P. Tian, F. Meng, H. Zhu, X. Jiang, X. Liu, P.K. Chu, Stimulation of bone growth following zinc incorporation into biomaterials, Biomaterials 35 (2014) 6882–6897.
[18] M. Long, H.J. Rack, Titanium alloys in total joint replacement — a materials science perspective, Biomaterials 19 (1998) 1621–1639.
[19] L. Saldana, A. Mendez-Vilas, L. Jiang, M. Multigner, J.L. Gonzalez-Carrasco, M.T. Perez-Prado, M.L. Gonzalez-Martin, L. Munuera, N. Vilaboa, In vitro biocompatibility of an ultrafine grained zirconium, Biomaterials 28 (2007) 4343–4354.
[20] J.R. Sin, A. Neville, N. Emami, Corrosion and tribocorrosion of hafnium in simulated body fluids, J. Biomed. Mater. Res. B 102 (2014) 1157–1164.
[21] W.A. Badawy, F.M. Al-Kharafi, The electrochemical behaviour of naturally passivated hafnium in aqueous solutions of different pH, J. Mater. Sci. 34 (1999) 2483–2491.
[22] Z. Cai, M. Koike, H. Sato, M. Brezner, Q. Guo, M. Komatsu, O. Okuno, T. Okabe, Electrochemical characterization of cast Ti–Hf binary alloys, Acta Biomater. 1 (2005) 353–356.
[23] Y.H. Jeong, H.C. Choe, W.A. Brantley, Corrosion characteristics of anodized Ti–(10–40 wt.%)Hf alloys for metallic biomaterials use, J. Mater. Sci. Mater. Med. 22 (2011) 41–50.
[24] Y.H. Jeong, K. Lee, H.C. Choe, Y.M. Ko, W.A. Brantley, Nanotube formation and morphology change of Ti alloys containing Hf for dental materials use, Thin Solid Films 517 (2009) 5365–5369.
[25] T. Kokubo, H. Takadama, How useful is SBF in predicting in vivo bone bioactivity? Biomaterials 27 (2006) 2907–2915.
[26] W. Jin, G. Wu, H. Feng, W. Wang, X. Zhang, P.K. Chu, Improvement of corrosion resistance and biocompatibility of rare-earth WE43 magnesium alloy by neodymium self-ion implantation, Corros. Sci. 94 (2015) 142–155.

[27] B. Sen, B.L. Yang, H. Wong, C.W. Kok, P.K. Chu, A. Huang, Effects of aluminum incorporation on hafnium oxide film using plasma immersion ion implantation, Microelectron. Reliab. 48 (2008) 1765–1768.
[28] Y. Zhao, G. Wu, H. Pan, K.W.K. Yeung, P.K. Chu, Formation and electrochemical behavior of Al and O plasma-implanted biodegradable Mg–Y–RE alloy, Mater. Chem. Phys. 132 (2012) 187–191.
[29] J.F. Moulder, W.F. Stickle, P.E. Sobol, K.D. Bomben, Handbook of X-ray Photoelectron Spectroscopy, Perkin-Elmer Corporation, Eden Prairie, 1992.
[30] G.L. Song, A. Atrens, Understanding magnesium corrosion — a framework for improved alloy performance, Adv. Eng. Mater. 5 (2003) 837–858.